THE ASTROPHYSICAL JOURNAL, 349:L1–L4, 1990 January 20

DETECTION OF SYSTEMATIC GRAVITATIONAL LENS GALAXY IMAGE ALIGNMENTS: MAPPING DARK MATTER IN GALAXY CLUSTERS

J. A. TYSON,[1,2] F. VALDES,[3] AND R. A. WENK[1]
Received 1989 July 19; accepted 1989 October 16

ABSTRACT

A gravitational lens distorts most background galaxies by stretching along a circle centered on the lens. This systematic alignment of 20–60 faint background galaxy images has been detected, centered on foreground galaxy clusters of high velocity dispersion. The background galaxy population is selected by its extreme blue $B-R$ color. At a limiting surface brightness of 29 B mag arcsec^{-2}, there are over 30 background galaxies arcmin^{-2} mag^{-1} anywhere in the sky, which is sufficient to map statistically the dark matter distribution in a foreground cluster. Pattern recognition software generates a two-dimensional lens distortion map. Initial results for the high-velocity dispersion clusters A1689 and CL 1409+52 are presented here. The dark matter is apparently correlated (center and radial extent) with the cluster red light, suggestive of a baryonic origin or dissipative coupling. The existence of a high percentage of lens-distorted faint blue galaxies sets a lower limit of approximately 0.9 to this background galaxy population mean redshift.

Subject headings: cosmology — dark matter — galaxies: clustering — galaxies: redshifts — gravitation

I. INTRODUCTION

Evidence for frequent gravitational lensing is mounting, with the recent discovery of several "arcs" (gravitationally distorted and highly magnified background galaxy images) in compact rich galaxy clusters (see Lynds and Petrosian 1989; Soucail *et al.* 1988, and references therein). A large blue arc occurs if a distant evolving galaxy falls near a point of infinite magnification (caustic) in the foreground lens. The arc in A370 has been analyzed by Lynds and Petrosian (1989) and Grossman and Narayan (1988). Lensed QSOs and bright arcs from caustics (as in A370) may be just the brightest examples of gravitational lensing.

At a limiting surface brightness of 29 B mag arcsec^{-2}, the sky is over 15% covered with a high surface density of faint blue galaxies: there are over 150,000 galaxies deg^{-2} between 26 and 27 B magnitude. This population has an unusually blue color near $B-R=0.3$. Several lines of evidence suggest that these galaxies are at redshifts between 1 and 3 (Tyson 1988; Guhathakurta, Tyson, and Majewski 1989). This distribution of distant galaxies is uniform over the sky to better than 10%. Foreground clumped mass will thus have a predictable systematic effect on the correlation of shapes of these background galaxies, even if they do not fall on caustics. Compared with galaxy–QSO lenses, the probability of galaxy-galaxy lensing is high. Automated detection of galaxy-galaxy lensing has been used to set limits to the dark halo of individual foreground galaxies (Tyson *et al.* 1984; Tyson 1987). In general, foreground galaxy clusters at redshifts 0.2–0.5 with radial velocity dispersions above 1000 km s^{-1} have sufficient mass density to significantly distort background galaxies of redshift greater than 1 (see Turner, Ostriker, and Gott 1984).

The 20–30 high-redshift background galaxies within the central square arcminute of a foreground compact cluster of galaxies will be lensed by the cluster mass distribution, creating faint arcs on scales of several arcseconds, selectable by their relatively blue color. These are not the comparatively rare caustic alignments: *every* background galaxy above some critical redshift will be seen as stretched along a circle centered on the lens. By going faint, the improved statistics of these distortions can help map the dark matter (DM) distribution, and thus constrain the nature of the DM. This new method is immune to the unbound galaxy contamination and dynamical assumptions in cluster virial mass estimates. With large numbers of lens-distorted galaxies, DM model fits are more unique.

Here we report the detection of multiple background galaxy gravitational lens distortions for two clusters of known high-velocity dispersion and X-ray luminosity: A1689 and CL 1409+52. A1689 ($z=0.18$), a richness class 4 cluster, has an X-ray luminosity of 1.7×10^{45} ergs s^{-1} (Jones and Forman 1990) and a radial velocity dispersion of 1800 ± 200 km s^{-1} (Gudehus 1989). CL 1409+52 ($z=0.46$) has an X-ray luminosity of 9.2×10^{44} ergs s^{-1} (Henry and Henriksen 1986) and a velocity dispersion of ~3000 km s^{-1} (Gunn 1989). These velocity dispersions must be taken as upper limits, due to possible contamination or subclustering.

II. OBSERVATIONS AND DATA PROCESSING

Eighty-five 100 s disregistered CCD exposures (47 in B_J and 38 in R) were obtained with the CTIO 4 m telescope on the cluster A1689 on 1989 February 6 UT. Cumulative 9600 B_J and 13,500 s R exposures on sparse fields were used to derive sky corrections for the raw CCD images. This in-field chopping technique is described by Tyson (1988). The CCD images cover a $4'\times4'$ field ($650\times650h_{75}{}^{-1}$ kpc at the cluster). Thirteen 500 s disregistered CCD exposures were obtained with the Canada-France-Hawaii Telescope on CL 1409+52 on 1988 May 19 and 21 UT, seven in the B_J filter and six in the I filter. Ninety-seven other disregistered exposures were obtained for sky flat data. The CCD images cover a $2'.1\times3'.4$ field ($630\times1020h_{75}{}^{-1}$ kpc at the cluster).

Preprocessing and FOCAS automated detection, splitting, and photometry reduced the multicolor images to a position-

[1] AT&T Bell Laboratories.

[2] Visiting Astronomer, CTIO, NOAO, operated by AURA, Inc., under contract to the National Science Foundation. Visiting Astronomer, Canada France Hawaii Telescope.

[3] National Optical Astronomy Observatories.

matched catalog (Tyson 1988). For the A1689 cluster field, 886 objects brighter than $27B_J$ mag were found in the 15 arcmin^2 area. There is an excess of 324 red objects in this area over that found in sparse fields. Due to the richness of this cluster, many of the faint blue galaxies (including some large blue arcs) are only revealed by subtracting a scaled R image from the B_J image. This removes much of the bright light of the cluster, permitting detection of faint blue objects. Figure 1 (Plate L1) shows the composite color image for the A1689 field. A tightly windowed monochrome image of $B_J - 0.35R$ is shown in Figure 2 (Plate L2). Lens-distorted background blue galaxies become mini-arcs along circles centered on the cluster lens. For the CL 1409 field, 476 objects were found to 27 B_J mag in the 5.4 arcmin^2 area in common between the B_J and I fields. Compared with survey fields there is an excess of 189 red galaxies ($B_J - I > 2.5$) brighter than 26.5 B_J mag associated with the foreground cluster.

III. GALAXY IMAGE LENS DISTORTIONS

Several faint arcs are seen in our blue images. However, the coherent alignment of the more numerous faint blue (background) galaxy ellipticities gives a stronger gravitational signal. The effect of a cluster gravitational lens is to stretch the apparent size of the image tangent to a circle centered on the lens. This stretch is measured using two scale lengths: the intensity weighted second moment of the galaxy image (part of the FOCAS catalog; Tyson *et al.* 1984, 1990) orthogonal and along the radius relative to the lens center. To detect the coherent stretching from the lens and cancel the intrinsic ellipticities of the galaxies, the scale lengths are averaged over the background population. From the two mean scale lengths, we form a dimensionless quantity similar to an ellipticity, which we call the net tangential alignment, and define as the difference of the scale lengths divided by the sum of the lengths. A random population of galaxies will give a net alignment of zero, while a population of lensed galaxies will give a value greater than zero.

To detect if a gravitational lens is present, the alignment statistic is computed using a grid of positions as candidate lens centers and the faint blue background galaxies with ellipticities >0.2 within 300 kpc of that point (the radius is arbitrary and not critical). A real lens produces an alignment value which is a maximum at the true center. Figure 3 (Plate L3) shows the alignment values for the cluster A1689 displayed as an image with brightness proportional to the tangential alignment strength. The best value for the center of the lens in A1689 is close to the red intensity centroid (shown with a cross in Fig. 2), and for CL 1409+52 the center is within 4″ of 3C 295. The area searched was 15 arcmin^2 for A1689, and 5.3 arcmin^2 for CL 1409+52. The alignment strengths at the lens centers are highly significant (>99% likelihood) as determined by comparison to a large number of random fields created by randomizing the sample galaxy positions without changing their measured shapes.

Using the lens centers determined above, we can study the alignment strength as a function of radius and compare it to the light distribution. The alignment statistic is computed using galaxies at various radii from the cluster center. Figure 4 shows the cluster red luminosity profiles compared with the alignment strength of faint blue galaxies in these two clusters. Log red intensity versus log radius is plotted along with the radial dependence of the lens image distortion.

The gravitational image distortions appear to extend radially at least as far as the cluster red light. The lens distortions are roughly correlated with cluster red light both in central position and radial extent. Note also the similarity between the image produced from the lens alignment statistic (Fig. 3) and the broad cluster red light distribution. These similarities imply that the dark matter distribution follows the *smoothed* cluster luminosity, with most of the mass interior to $100h_{75}{}^{-1}$ kpc.

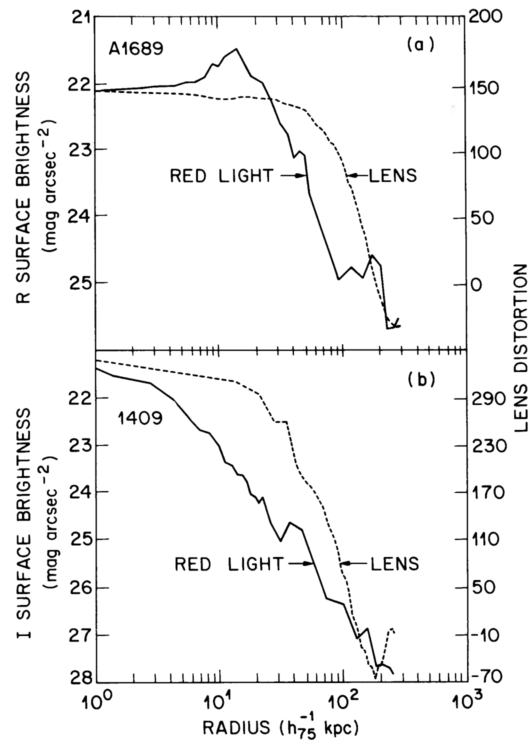

FIG. 4.—Cluster red luminosity profiles compared with strength of tangential alignment of faint blue background galaxies. Observed log red intensity vs. log radius is plotted along with the radial dependence of the net tangential alignment. The I band at the higher redshift of 1409+52 is equivalent to the R band at the redshift of A1689. These two clusters differ in angular size by a factor of 1.8. Note that the gravitational image distortions follow the red cluster light, smoothed over about 100 kpc.

Histograms of faint galaxy alignments (45° bins) relative to the cluster centers, and many control fields, are shown in Figure 5. Faint blue galaxies and faint red (virtually all cluster) galaxies are distributed very differently in alignment. Figures 5*a* and 5*b* show the relative alignment for the blue and red galaxies in the field A1689. The blue/red subsamples were defined by the color-magnitude diagram for the field by noting the segregation in $B_J - R$ color into two groups. For A1689 blue = $B_J - R < 0.7$ (Fig. 5*a*), and red = $B_J - R > 1$ (Fig. 5*b*). For CL 1409, blue = $B_J - I < 2$ (Fig. 5*c*), and red = $B_J - I > 2.5$ (Fig. 5*d*). The apparent magnitudes are in the range 22–26 B_J mag, out to the maximum radius from the cluster center permitted by the image: $330h_{75}{}^{-1}$ kpc for A1689, and $250h_{75}{}^{-1}$ kpc for CL 1409+52. Our simulations produce similar alignment histograms, showing that noise and seeing cause some faint tangentially aligned background galaxies to scatter into other alignment bins. A null result from the sum of 11 control fields, each with a surveyed area similar to that of our CL 1409 data, is shown in Figure 5*e*. Statistical significance of the lens alignments (7–10 σ per cluster) and particularly the integral distortion statistic are high.

This systematic lens distortion is not possible for back-

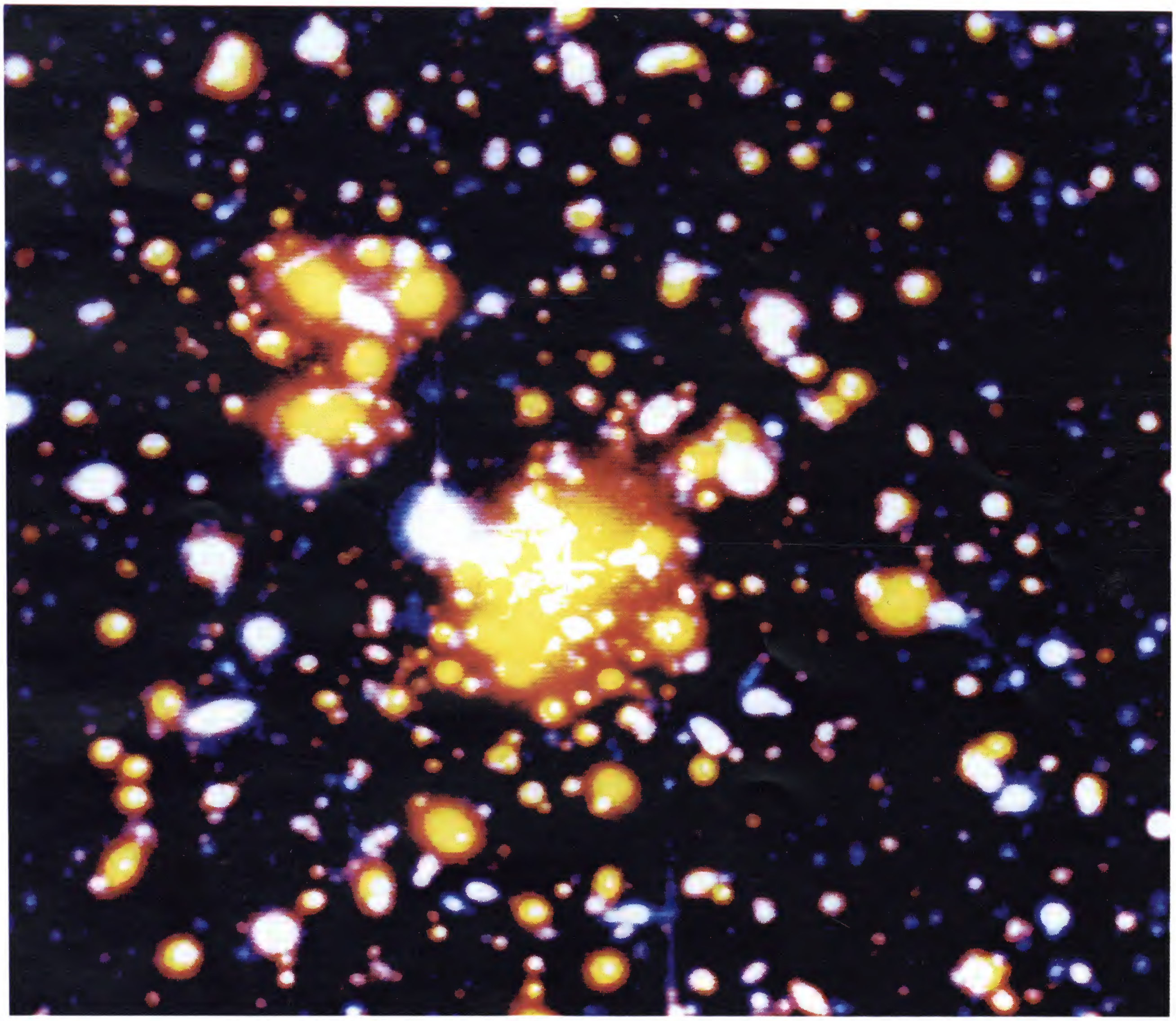

FIG. 1.—A composite color image of the A1689 field [red, green, blue] = [R, B_J, $B_J - 0.35R$]. Lens-distorted background blue galaxies become arcs and mini-arcs along circles centered on the cluster lens.

TYSON, VALDES, AND WENK (*see* **349**, L2)

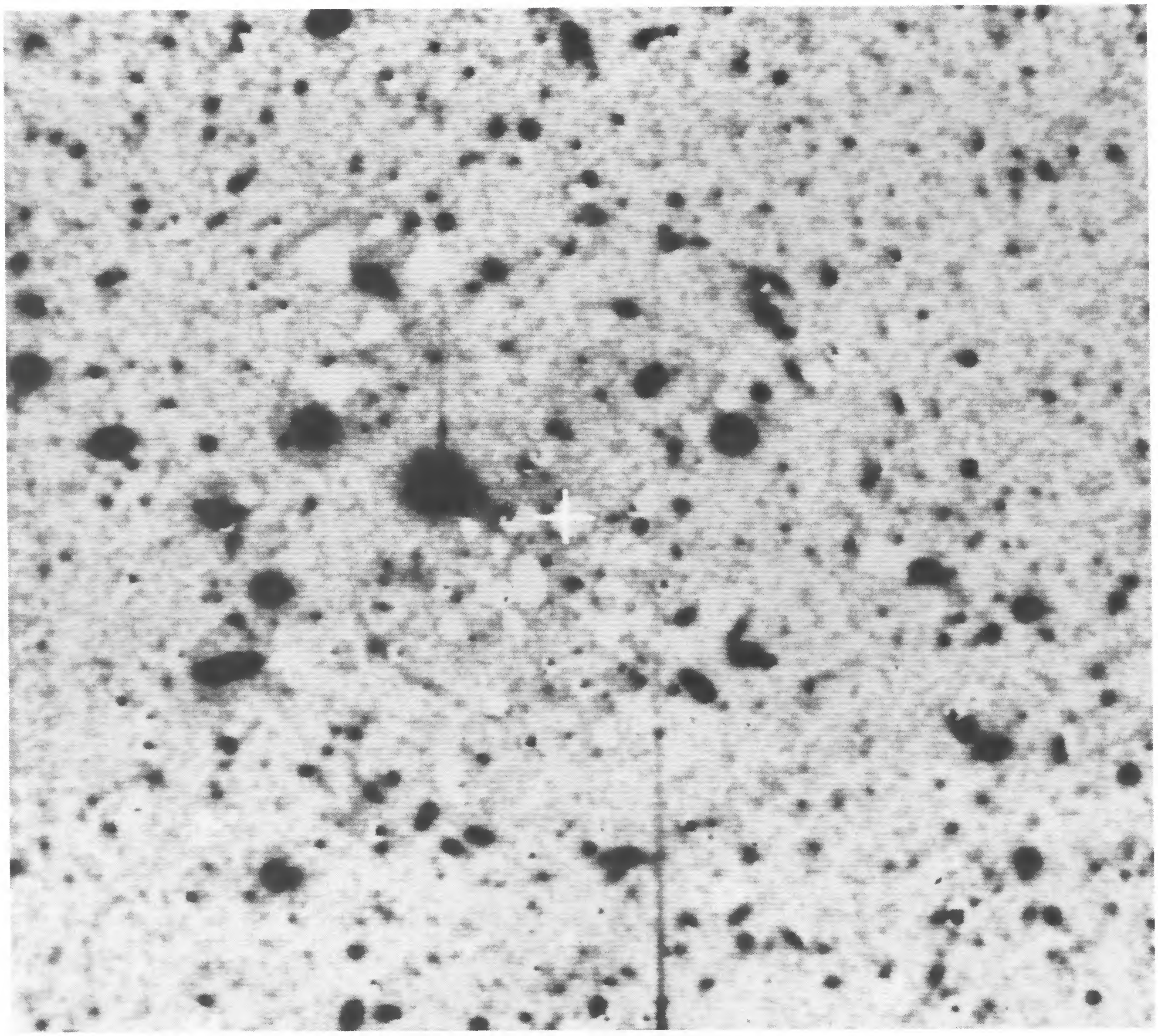

FIG. 2.—The monochrome blue image of A1689 with a scaled red image subtracted to eliminate much of the cluster light [$\log(B_J - 0.35R)$]. Several large blue arcs are seen. However, the coherent alignment of the more numerous faint blue (background) galaxy major axes gives a stronger signal. In this 3'.8 × 4' field over 50 lens-distorted galaxy images are also stretched along circles about the lens center. The cross is centered on the brightest cluster galaxy.

TYSON, VALDES, AND WENK (*see* **349**, L2)

1990ApJ...349L...1T

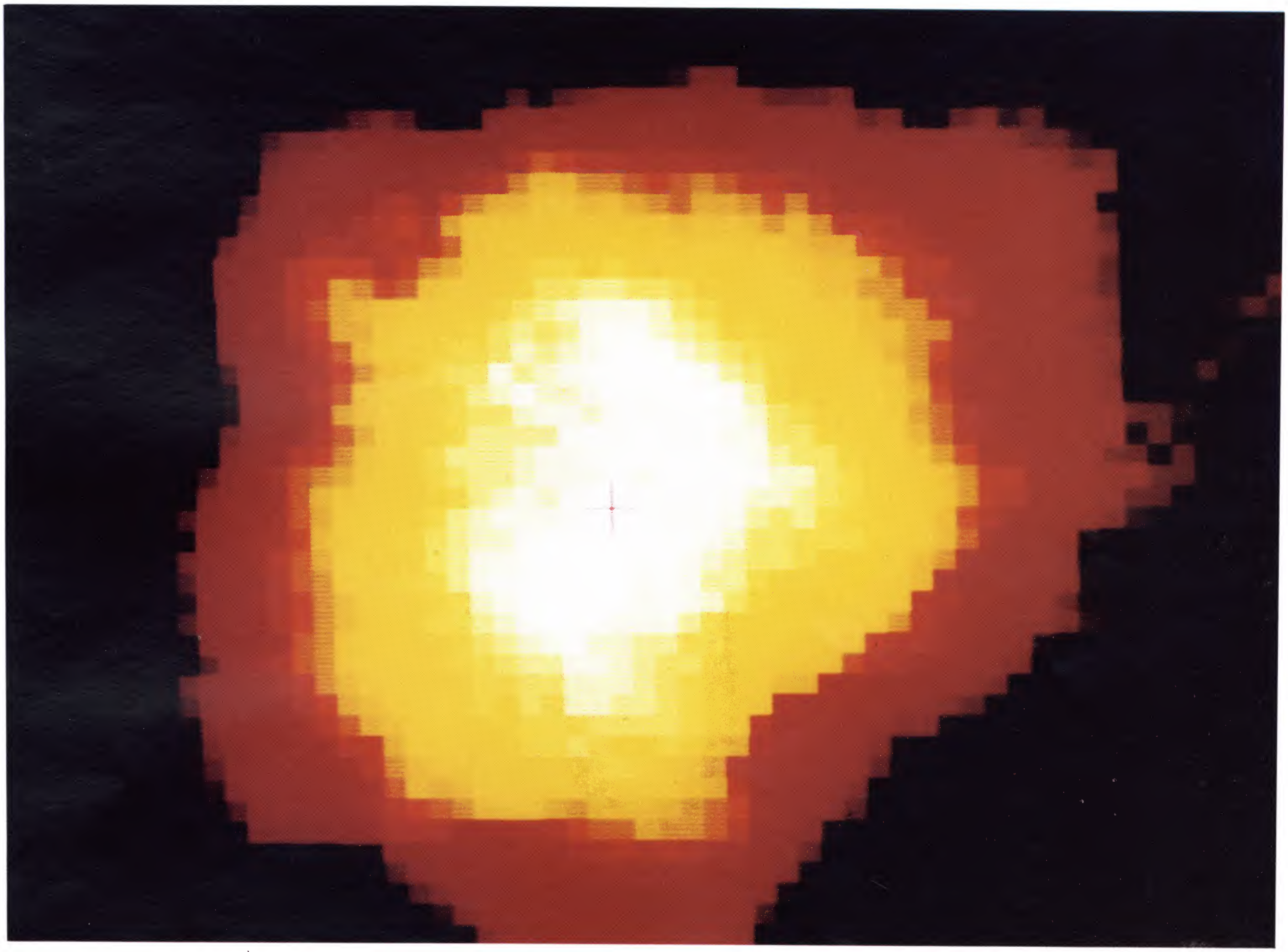

FIG. 3.—A pseudocolor image of the lens in A1689. The net tangential alignment of 22–26 *B* mag blue galaxies is shown. The resolution for this image is 3″, and the orientation and scale are the same as Figs. 1 and 2.

TYSON, VALDES, AND WENK (*see* **349**, L2)

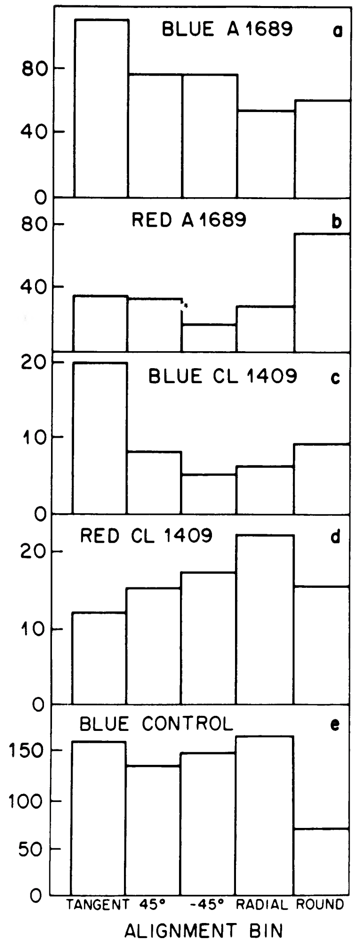

FIG. 5.—Histograms of faint galaxy major axis alignments relative to the vector to the cluster center are binned (for ellipticities above 0.2) into four orientations: tangent (90°), radial (0°), and ±45°. Only galaxies of 22–26 B_J mag are included. An excess number of blue galaxies are aligned orthogonal to the radius of the cluster center (tangent bin), due to the lens distortion. Blue (background) and red (cluster) galaxy alignments for the A1689 field are shown in Figs. 5*a* and 5*b*, and for CL 1409+52 in Figs. 5*c* and 5*d*. Figure 5*e* shows the faint blue galaxy alignment histogram for the sum of 11 similar high-latitude comparison fields with no foreground clusters.

ground galaxies below a critical redshift, depending on the lens mass and redshift (Turner, Ostriker, and Gott 1984): an unreasonably large mass for the lens would be required. Outside the cluster core, the area density of aligned blue galaxies found in the $z = 0.46$ cluster 1409+52 field is nearly equal to the number of blue galaxies found in deep sparse field surveys (Tyson 1988). There are a total of 27 blue galaxies in the 1.4 arcmin^2 area covered by the alignment histogram sum for the $z = 0.46$ cluster 1409+52. Thirty-five blue galaxies in the 22–26.5 B_J mag range would have been expected, based on deep surveys. From the fractional excess in the tangent alignment bin, and lens simulations described below, we conclude that at least 70% of these faint blue galaxies have redshifts larger than 0.9. Similar studies of other clusters with redshifts 0.6–1 will help map the field galaxy density as a function of redshift in the interesting region $1 < z < 3$.

IV. SIMULATIONS

We have simulated cluster lens distortions of background galaxies, by ray-tracing real images, as a function of cluster and DM parameters and compared them with the observations (Tyson *et al.* 1990). The background galaxy fields are taken from actual deep sparse field imaging on the same observing run. These data are processed so that the noise is identical to that on the real cluster images. These background galaxies are assigned redshifts in three model schemes: all at $z = 1$, all at $z = 2$, and equally at $z = 1$ and 2. The cluster galaxies (found by their color, brightness, or redshifts) are assigned truncated isothermal mass distributions obtained from individual galaxy surface photometry to 28 B_J mag, *K*-corrections derived from the observed colors, and the Faber-Jackson relation $\sigma_V = 220$ dex $[(20.2 - B_J)/10]$. For any reasonable assigned galaxy mass distribution these cluster galaxies make a small contribution to the background galaxy image distortions beyond several arcseconds from the cluster galaxies. Finally a soft core isothermal mass distribution is superposed on the cluster galaxies. The velocity dispersion (500–2500 km s^{-1}) and core half-surface-density radius (25–100$h_{75}{}^{-1}$ kpc) are varied.

To relate the observations to the simulations the net tangential alignment of background galaxies over the extent of the cluster is computed for both the observations and the simulations in exactly the same way (including FOCAS processing). The alignment strength is found to be proportional to the radial velocity dispersion and weakly dependent on DM core size ($R_{\rm core} < 100h_{75}{}^{-1}$) and the background redshift ($z_{\rm bg} > 1$). We have examined distortion statistics $D_1(r) = (a - b)/(a + b)$ and $D_2(r) = (a^2 - b^2)/(a^2 + b^2)$ (plotted in Fig. 4), where a and b are sums over faint blue galaxies of the major and minor axes of the principal axis (r, θ) transformed moments. For velocity dispersions $500 < \sigma_v < 1800$ km s^{-1}, the integral over radius of this distortion statistic is proportional to the velocity dispersion and weakly dependent on DM core size ($R_{\rm core} < R_{\rm Einstein}$). The best agreement with the observed lens statistics for CL 1409+52 is obtained for $25 < R_{\rm core} < 50h_{75}{}^{-1}$ kpc, $\sigma_{V,\rm DM} =$ 1100–1500 km s^{-1}, for $z_{\rm bg} = 2$. Results for the A1689 simulations are similar: $\sigma_{V,\rm DM} = 1200$–1500 km s^{-1}. These 2 σ ranges are from the scatter between simulations and core trends. Note these "DM" parameters refer to all mass, dark+luminous, *other* than that associated with the 14 (CL 1409) and 44 (A1689) modeled brighter cluster galaxies. These and other DM lens model simulations will be shown in detail elsewhere (Tyson *et al.* 1990). Attempts to account for the observed cluster lens distortions by assigning arbitrarily large masses to as many as 50 of the brightest observed cluster galaxies failed: massive diffuse DM in the inner $200h_{75}^{-1}$ kpc is needed. Our technique is relatively insensitive to a gentle outer mass cutoff at radii larger than $300h_{75}^{-1}$ kpc. Abrupt outer cutoffs, however, as is seen in the A370 cluster lens data, are detectable.

V. SUMMARY

Limits to the DM distribution can be set by studying the distribution of image distortions, relative to the cluster center, of background galaxies selected by their extreme blue colors. It is necessary to reach a limiting surface brightness of at least 28 B_J mag arcsec^{-2} to obtain a sufficient area density of background galaxies. At 29 mag arcsec^{-2}, the background galaxies are resolved, and seeing affects measured distortion only weakly.

Comparison with models for the cases of A1689 and CL 1409+52 indicates the need for a soft core dominant DM component with about 1100–1500 km s^{-1} radial velocity dispersion for the dark component, depending on the DM core size. Based on these initial clusters, we find that the DM distribution is similar to the smoothed red cluster light. This is consistent with baryonic DM or baryonic-nonbaryonic dissipative coupling. A study of a large sample of galaxy cluster fields can constrain the nature of the dark matter.

We are grateful to A. Cronin, P. Guhathakurta, C. Christian, P. Waddell, and P. Boeshaar for help with some of the observing and data preprocessing. We had helpful discussions with E. Turner, J. Gunn, J. Huchra, B. Fort, Y. Mellier, and C. Jones. A. Penzias and E. Turner commented on an earlier manuscript. The observational program is part of a more general international collaboration (B. Fort, G. Soucail, Y. Mellier, and E. Turner) to study blue arcs in clusters by spectroscopy and imaging.

REFERENCES

Grossman, S. A., and Narayan, R. 1988, *Ap. J. (Letters)*, **324**, L37.
Gudehus, D. 1989, *Ap. J.*, **340**, 661.
Guhathakurta, P., Tyson, J. A., and Majewski, S. 1989, *Ap. J.*, in press.
Gunn, J. E. 1989, in *The Epoch of Galaxy Formation*, ed. C. S. Frenk (Dordrecht: Kluwer), in press.
Henry, J. P., and Henriksen, M. J. 1986, *Ap. J.*, **301**, 689.
Jones, C., and Forman, W. R. 1990, *Ap. J. Suppl.*, in press.
Lynds, R., and Petrosian, V. 1989, *Ap. J.*, **336**, 1.
Soucail, G., Mellier, Y., Fort, B., Mathez, G., and Cailloux, M. 1988, *Astr. Ap.*, **191**, L19.
Turner, E. L., Ostriker, J. P., and Gott, J. R., III. 1984, *Ap. J.*, **284**, 1.
Tyson, J. A. 1987, in *Theory and Observational Limits in Cosmology*, ed. W. R. Stoeger (Vatican City: Specola Vaticana), p. 441.
———. 1988, *A.J.*, **96**, 1.
Tyson, J. A., Valdes, F., Jarvis, J. F., and Mills, A. P. 1984, *Ap. J. (Letters)*, **281**, L59.
Tyson, J. A., Valdes, F., Wenk, R. A., and Cronin, A. 1990, in preparation.

J. A. Tyson and R. A. Wenk: AT&T Bell Laboratories, 1D335, Murray Hill, NJ 07974

F. Valdes: KPNO-COM, P.O. Box 26732, Tucson, AZ 85726